Code-Empowered Lightwave Networks

Camille-Sophie Brès, *Student Member, IEEE*, and Paul R. Prucnal, *Fellow, IEEE*, *Fellow, OSA*

***Abstract*—In this paper, an architecture for code-empowered optical CDMA (OCDMA) lightwave networks is presented. The architecture is based on reconfigurable optically transparent paths among users of the network to provide high-bandwidth optical connections on demand over small areas such as local area networks or access networks. The network operates on the transmission of incoherent OCDMA codes, each network station being equipped with an OCDMA encoder and decoder. The routing at a network node is based on the OCDMA code itself. The destination address, as well as the next node on the path, is given by the code as in a code-empowered network. A node consists of an OCDMA router built from parallel code converter routers that perform switching, routing, and code conversion. The latter enables a virtual code path for increased scalability. Commonly available delay lines enable the tunability of the encoder, decoder, and router for a reconfigurable and flexible network. Flexibility and granularity are also accentuated by OCDMA encoding. An OCDMA lightwave network can therefore respond to changes in traffic load, traffic conditions, failure, and other network impairments. We describe the possible architectures and the routing constraints of such OCDMA lightwave networks. We present a power analysis and focus on the performance issues of dynamic routing. The effect of coding, topology, load condition, and traffic demand is analyzed using simulations. The obtained results show that the flexibility of OCDMA and the large offered cardinality can be a solution to the needs of local area and access networks.**

***Index Terms*—Code division multiaccess, local area networks, optical fiber communication, routing.**

I. Introduction

THE LAST few decades have seen a phenomenal growth in telecommunication-based services, which have been driven primarily by the Internet. As the expansion of the Internet continues along an unpredictable path, many new applications are foreseen and expected, placing increasing demands for ultrascalable, flexible, transparent, high-speed, and dedicated bandwidth services. Driven by these demands and nature of traffic, optics is now beginning to expand from a core technology toward the metro and access networks. Access networks are characterized by a large diversity in terms of protocols, services, infrastructures, transmission rates, and clients. The customer base is very broad and spans from individual users all the way to enterprises and large corporations. Overall, access networks are very dynamic and unpredictable. Customers are looking for inexpensive and transparent solutions for the development of efficient new access networks. Optical schemes, which are able to provide dedicated high-bandwidth connections to individual users, are being actively explored.

Optical CDMA (OCDMA), with advantages such as simplified control, random access to the entire bandwidth, and flexible bandwidth allocation [1], is a good candidate for local area networks [2], [3]. OCDMA can be divided into two main branches: coherent and incoherent approaches. The former applies a code via phase encoding of the optical signal field and recovers the data via phase detection. The latter uses the more standard technique of intensity modulation with direct detection. The most common approaches to incoherent OCDMA are based on spectral-amplitude coding [4], spatial coding [5], temporal spreading [6], and 2-D wavelength-hopping time-spreading (WHTS) coding [7]–[9]. Coding in multiple dimensions, such as spectral amplitude and WHTS, adds more flexibility while increasing the capacity and performance. In this paper, we focus on 2-D incoherent WHTS architectures.

Incoherent OCDMA presents robustness to environmental conditions, nonlinearity, and coherent effects and utilizes commercial off-the-shelf components. Multihop networks require good granularity as well as tunability. Tunability is key if the network is to respond rapidly in case of failure or changes in load conditions in order to maintain a specific throughput and performance level. Robustness is also preferable: the signals propagate through multiple hops and need to maintain the information, which is complex if the information is contained in the phase. Considering the stringent requirements for multihop networks, incoherent OCDMA therefore appears to be a good candidate. Building a code-empowered network could also allow shifting some of the network management functions, such as quality of service or congestion control, to the physical layer of the network.

This paper is organized as follows. Section II gives an overview of the network architecture, covering network stations and router nodes. In Section III, we describe the routing rules related to coding and routing constraints. The network performance, power budget and simulations, is covered in Section IV. Finally, the discussion and conclusions are presented in Section V.

II. Network Architecture

A. Overview

An OCDMA lightwave network consists of network stations connected by a network of nodes (Fig. 1). The network stations are equipped with OCDMA transmitters and receivers. A data signal travels from the sending station to the receiving station by going through one or a series of nodes. The routing nodes

Manuscript received November 5, 2006; revised July 5, 2007.

C.-S. Brès is with the Department of Electrical Engineering, Princeton University, Princeton, NJ 08544 USA, and also with the Department of Electrical Engineering, University of California, San Diego, La Jolla, CA 92093 USA (e-mail: cbres@ece.ucsd.edu).

P. R. Prucnal is with the Department of Electrical Engineering, Princeton University, Princeton, NJ 08544 USA (e-mail: prucnal@princeton.edu).

Color versions of one or more of the figures in this paper are available online at http://ieeexplore.ieee.org.

Digital Object Identifier 10.1109/JLT.2007.904934

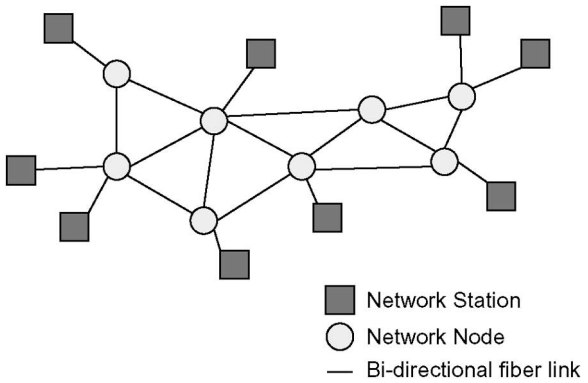

Fig. 1. Schematic of a multihop network.

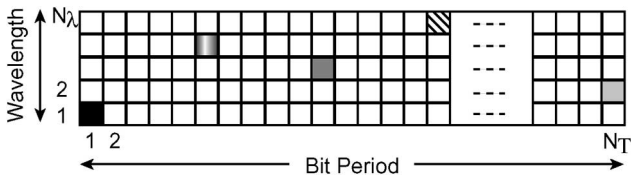

Fig. 2. Matrix representation of a 2-D incoherent code.

direct the traffic through the network: the individual signals are routed depending on the OCDMA codes they carry, the destination address being the OCDMA code itself. Bidirectional links connect the network.

B. Network Station

An OCDMA transmitter comprises of a light source, a modulator, and a 2-D WHTS encoder. The OCDMA receiver consists of a 2-D WHTS decoder having the same structure as its corresponding encoder, a thresholder and/or time gate, and a photodiode. In 2-D WHTS OCDMA systems, the pulses are encoded in both the time domain and the wavelength domain simultaneously: the codes can be represented as matrices with time and wavelength on the two axes. The wavelength domain is divided into N_λ channels of bandwidth δ_ν and the time domain into N_t time chips of duration τ_c. A code consists of w short pulses of different wavelength, where w is called the weight of the code, within the N_t available time chips. The 2-D representation of a code is given in Fig. 2. The most common codes typically have one pulse per row, as shown in Fig. 2. Some codes also use multiple pulse per row or multiple pulse per column approaches.

Most recent implementations of 2-D OCDMA utilize multiwavelength sources to avoid the need for sources that can rapidly wavelength hop. The pulses can be generated from an array of mode-locked lasers, which is limited in scalability due to the higher complexity in controlling a large number of lasers or from a broadband source. Various broadband sources have been used: light-emitting diodes, amplified spontaneous emission noise from erbium-doped fiber amplifier (EDFA), gain-switched Fabry–Pérot lasers, and supercontinuum generation [10]. The encoder essentially creates a combination of two patterns: a wavelength-hopping pattern and a time-spreading pattern. Some implementations perform the two patterns independently like array waveguide gratings (AWGs) or thin-film filters (TFFs) [11], or simultaneously as fiber Bragg gratings (FBGs) [12], holographic Bragg reflectors (HBRs) [13], or chirped Moire gratings (CMGs) [14]. Four possible encoder designs for four wavelengths, using AWGs, TFFs, or FBGs, are shown in Fig. 3. The optical delay lines allow the encoder to be tunable: the position of the wavelengths within the bit interval can be changed in order to create a different code from the same code family. We define a code family as the total number of valid codes ϕ, which is also called the cardinality, that can be obtained with the same N_λ wavelengths and N_T chips. A valid code has to satisfy specific values of cross and autocorrelation. The fourth design, using FBGs, is shown for illustration. Encoders based on FBGs, HBRs, or CMGs are not as tunable as the one based on filter technologies. The wavelengths can be temperature-tuned, but not the time delays, limiting their tunability.

For all three architectures, the wavelengths are first separated using the AWG or the TFFs. In the cascade architecture [Fig. 3(b)], the reflected ports of the filters are used to connect the filters together. The wavelengths are then independently delayed, allowing the use of tunable optical delay lines for dynamic variation of codes. Depending on the required speed of tuning, manual delay lines, integrated delay lines [15], or serial delay lines [16], [17], tuning in hertz, kilohertz, and gigahertz, respectively, can be implemented. The wavelengths are therefore positioned in a specific time chips and are then recombined to form a code.

While an encoder spreads the wavelengths in time over the bit period, the delay lines of the encoder are set to "de-spread" a specific code: the wavelengths are realigned in time to create an autocorrelation peak of height w. All other codes that are not matched to the receiver will be further spread to create a cross-correlational noise called multiple access interference (MAI). All OCDMA systems are primarily limited in their performance by MAI [18]. In order to eliminate this noise, the dominant source of bit errors in an OCDMA network, a thresholder, or time gate, such as a terahertz optical asymmetric demultiplexer (TOAD) or a nonlinear optical loop mirror [19]–[22], follows the decoder: All signals falling below the threshold or outside the time window containing the autocorrelation peak will be eliminated before detection.

When network station A requests to transmit to station B, this being defined as a call, a network control unit predetermines a path for that call, if a path is available. A channel is then assigned to the call. The data are put on the channel and sent on the network. In the following section, the routing as well as the availability of paths will be covered in more detail.

C. Router Node

The router node receives multiplexed OCDMA data channels, the network traffic. The various data channels are directed to the intended router output, depending on their assigned path. The signals thus travel through the network from node to node until they reach their final destination. The main building block of the router node is a code converter router described in Fig. 4 [23].

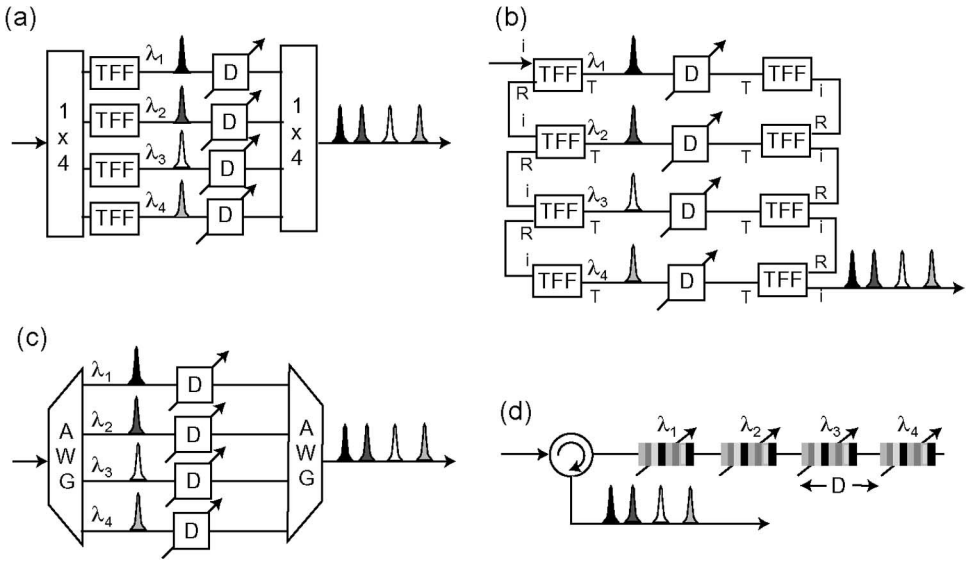

Fig. 3. Two-dimensional OCDMA encoder/decoder architectures. (a) Parallel TFFs, (b) cascaded TFFs, (c) AWGs, and (d) FBGs. D: Delay line, i: Input port, R: Reflected port, and T: Transmitted port.

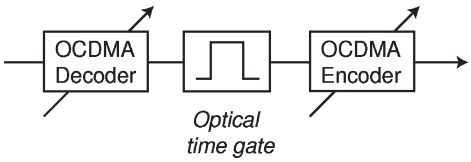

Fig. 4. Two-dimensional OCDMA code converter.

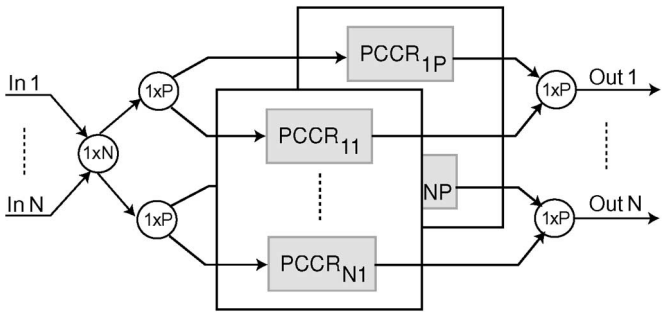

Fig. 5. Two-dimensional OCDMA router node.

Each code converter router consists of a tunable decoder, to select one of the input codes, an optical gate to sample the bit and retrieve the autocorrelation peak consisting of w wavelengths, and a tunable encoder to re-encode the data to be sent on the next link. Similar to the network stations, the tunability can be achieved by optical delay. Since this type of network is mostly designed for circuit switching, the encoders and decoders can be slowly tuned, loosening the constraint on delay line speed.

The router node, as shown in Fig. 5, utilizes the code converter routers in parallel [parallel code converter routers (PCCRs)]: each of the PCCRs is preconnected to a specific output and performs routing by selecting a specified code from the incoming broadcast traffic. The node has N inputs and N outputs, where N is the degree of the node. A star coupler directs the combined incoming traffic to all the PCCRs and up to P. PCCRs are combined back at one output link. For

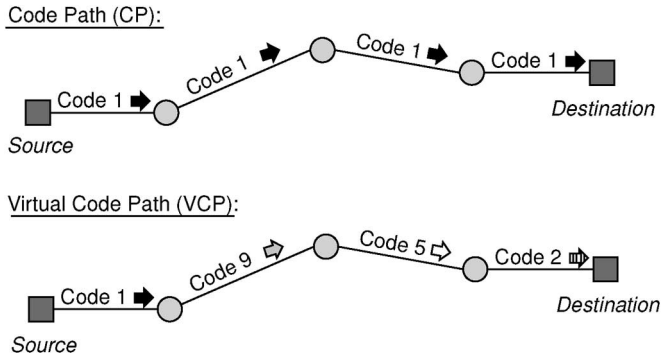

Fig. 6. CP and VCP.

example, the PCCRs for output 1 are shown as PCCR_{11} to PCCR_{1P}, where PCCR_{ij} corresponds to user j being directed to output i. The maximum number of channels that can be multiplexed on one output link is therefore P. The decoder/gate combination performs code selection and routing. The encoder performs code assignment. The output code can be set to the input code; in this case, the channel uses one and only one OCDMA code along the path, and the network performs code path (CP). However, since this encoder is tunable, the incoming code can be converted to any other code in the same code set, and an OCDMA code can be assigned on a link by link basis. In this case, the channel uses different OCDMA codes along the path, and the network performs virtual CP (VCP). The illustration of CP and VCP is shown in Fig. 6 for a signal going from source to destination with three hops (i.e., four links).

This transparent all-optical router does not require light sources or optical-electrical-optical conversion and can be scaled by adding PCCR modules. Increased network flexibility is achieved by the VCP, creating a larger effective number of codes and more potential users, while simplifying the routing. This 2-D WHTS OCDMA router was experimentally demonstrated in [23].

III. Routing Constraints

As mentioned previously, the network control unit looks for an available path for a requested call. If a path is available, the control unit then establishes the connection by properly setting the tunable encoders and decoders within the router nodes to create a CP or VCP from source to destination. Once all encoders and decoders along the path are set, a circuit is ready to be used by the requesting station. While static routing is simpler to implement and does not require reconfigurability, it cannot respond to changes in load patterns or link failure. OCDMA presents advantages such as flexibility and tunability, which, in turn, enable dynamic routing; the path connections are thus not hardwired: information about the various calls in progress is used to optimize the performance of the network. The coding features of OCDMA and its soft-blocking characteristic impose specific constraints and rules on path availability, allocation, and routing of signal within the OCDMA path network.

A. Coding

The family of incoherent 2-D codes implemented at the network station will have an impact on the system performance. Various encoding methods have been proposed for WHTS schemes. Common families of codes are carrier-hopping prime codes (CHPCs) [24], prime hop codes [25], Yu/Park codes [26], and extended CHPC [27]. The combination of the number of wavelengths (N_λ), which is chosen in accordance with the amount of bandwidth available, the weight of the code (w), and the number of time chips (N_T), related to the bit rate (R) and the width of the optical pulse (τ_p), determine the performance metrics of the code. For an OCDMA network, the metrics of interest are the cardinality ϕ and the number of simultaneous users K tolerated at a specified fixed BER. An important feature of any OCDMA codes is their soft-blocking characteristic. In wavelength division multiplexing (WDM) systems, once all available wavelengths are used (one wavelength per user), no more users can be added on the network. There is a hard limit on the number of users set by $K \leq N_\lambda$, where K is independent of BER. OCDMA can trade off a number of users for performance. This soft-blocking behavior of 2-D OCDMA codes is illustrated in Fig. 7 where the probability of error (P_e) is plotted versus the number of simultaneous users for $N_\lambda = w = 8$ and $N_T = 101$ (8, 8, 101) CHPC. The upper bound of P_e for the CHPCs can be expressed with an exact analytical expression and facilitates the understanding of system performance. For a network with K simultaneous users, an error occurs when cross-correlational pulses from the $(K-1)$ interfering users built up to a level higher than the autocorrelation peak changing a bit "0" in a bit "1." The cross correlation of CHPCs is bounded by 1. A parameter q, which is called the hit probability, is used to describe this overlap probability and is given by $q = w/2N_T$. The expression for P_e is [24]

$$P_e = \frac{1}{2}\sum_{i=w}^{K-1}\binom{K-1}{i}(q^i)(1-q)^{(K-1-i)}. \quad (1)$$

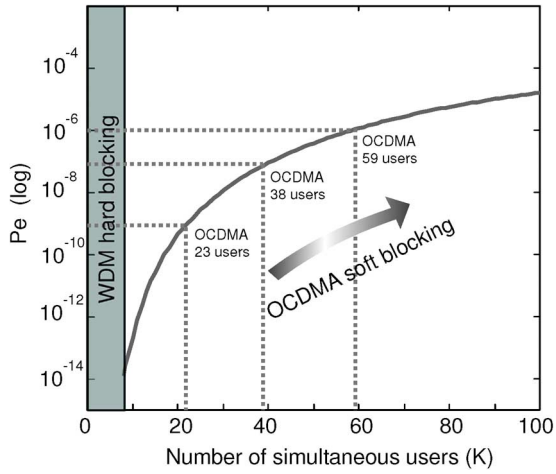

Fig. 7. P_e versus K for (8, 8, 101) CHPCs. Soft and hard blocking.

If the lowest BER tolerated is 10^{-9}, up to $K = 23$ users can be multiplexed for this system. If some more flexibility in the BER is acceptable, such as 10^{-6}, more users $(K = 59)$ can be accommodated simultaneously. We can note that, with the same number of wavelengths, more users can, in general and depending on the codes, be supported with OCDMA compared to WDM. The only constraint is the cardinality: there cannot be more stations on the network than the number of codes available. This number is typically very large and should not be a limiting factor for the type of local area networks considered. In summary, the choice of the code family, the combination of (w, N_λ, and N_T), and the specific BER performance required on the network result in two main parameters: cardinality ϕ and the number of simultaneous users K.

B. Routing Rules

The code parameters (ϕ and K) and the incoherent decoding scheme impose two main routing requirements: distinct code assignment and link occupancy. When a call is placed, the network control unit looks for a path that fulfills those requirements. If no path is found, the call is rejected. If a path is found, the call is granted, and the connection is established.

1) Distinct Code Assignment: When the multiplexed traffic arrives at an OCDMA decoder, it is necessary that no identical codes should be present: in order to distinguish two different data streams at a decoder, they must be carried on different OCDMA codes. Considering the router nodes, if S streams of data sent on the same code reach a common node, the information on all S streams will be corrupted due to the broadcast architecture of the router node. Therefore, the distinct code assignment, which is a distinct wavelength assignment in a WDM network, is important to ensure correct operation of the network. It is also necessary that no identical codes should be sent on the same link for the same reasons stated above. Therefore, there are two requirements: distinct code per router (DCPR), with no identical codes reaching the same node, and distinct code per link (DCPL), with no identical code sent on a link. These distinct code assignment conditions can be summarized as follows: let router R_j have N neighbors

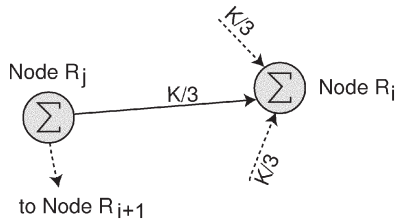

Fig. 8. Link occupancy constraint for OCDMA networks.

$R_i (1 \leq i \leq N)$, i.e., there is a link between R_i and R_j. Let C_{ij}^r be an OCDMA code r sent from R_i to router R_j, with $1 \leq r \leq W_i^{\max}$, and $W_i^{\max}$ being the maximum number of codes that can be multiplexed on the link i entering node R_j; $W_i^{\max}$ is called the maximum weight of the link. Then

$$C_{ij}^r \neq C_{(i+1)j}^r, \quad 1 \leq i \leq (N-1) \tag{2a}$$

$$C_{ij}^r \neq C_{(i)j}^{r+1}, \quad 1 \leq r \leq (R-1). \tag{2b}$$

Equation (2a) represents the DCPR constraint, while (2b) represents the DCPL constraint.

2) Link Occupancy: As mentioned in the previous section, an important metric for OCDMA networks is K, which is the maximum number of simultaneous codes allowed for a required BER. If more than K codes arrive at an OCDMA decoder, the level of MAI will be higher than tolerated: this will lead to an undesired decrease in performance. In order to prevent this type of degradation, the network must ensure that K or fewer codes are convergent on a router node. Due to the broadcast operation performed at the input of the router, the total capacity entering the node must be less than K, as described in (3). We recall that W_i is the number of codes on link i

$$\sum_{i=1}^{N} W_i \leq K. \tag{3}$$

This link occupancy condition can be related to the number P (see Fig. 5) of possible parallel branches (PCCRs) in the router node and the degree of the neighbor nodes, $P \leq (W_i^{\max})$. Up to now, for simplification, we have assumed that P is the same for all links, i.e., all nodes have the same degree. This does not need to be always the case as some node could have more inputs than others. However, we assume that a node degree is relatively low and even across all nodes, which is an accurate assumption for small multihop networks. In our simulations, we also assume that the traffic is random, all links having the same probability of being used. Therefore, we assume that the total tolerable input traffic K is evenly distributed over all input links, as shown in Fig. 8. If K and N are not multiples, the value is rounded down, and the remaining available codes can be used on any of the N link until the value of K is reached.

Fig. 8 shows two neighboring nodes: R_i and R_j. Node R_i has a degree of three: the weight on the three input links is therefore $K/3$. The weight on the output links depends on the degree of the neighboring nodes. As a reminder, the cardinality ϕ is usually much larger than K. P can now be related to K and N: $P \leq K/N$.

TABLE I
NETWORK PARAMETERS

P_{tx}	Source signal power
P_{rx}	Received signal power
L_{enc}	Encoder loss
L_{dec}	Decoder loss
L_{link}	Loss due to fiber and connections
L_{split1}	Loss at the input of the router node due to splitting
L_{split2}	Loss at the output of the router node due to splitting
L_{hop}	Total loss between 2 nodes
G_{amp}	Link optical amplifier gain
N_{hop}	Number of hops

C. Discussion

Since multihop networks typically do not have high node degree, the distinct code assignment condition will not limit the performance: the network control, by managing the assignment of OCDMA codes on the network links, can easily ensure that the code assignment condition is not violated. This is different for WDM networks or linear lightwave networks where some link cannot be used due to wavelength conflicts even if they are not fully occupied. We can now define blocking of a call: a call is blocked exclusively when the number of users asking for a link is higher than its maximum allowed weight $W_i^{\max}$.

IV. NETWORK PERFORMANCE

In this section, we look at some network requirements and limitations by analyzing the power budget constraints. An analytical analysis of the power budget is first presented. The network performance is then studied using a simulator.

A. Power Budget Analysis

The network parameters used in our power budget analysis are summarized in Table I.

The power at the receiver can be computed as follows:

$$P_{\mathrm{rx}} = P_{\mathrm{tx}} - L_{\mathrm{enc}} - N_{\mathrm{hop}} L_{\mathrm{hop}} + N_{\mathrm{hop}} G_{\mathrm{amp}} - L_{\mathrm{dec}} \tag{4}$$

$$P_{\mathrm{rx}} = P_{\mathrm{tx}} - N_{\mathrm{hop}} (L_{\mathrm{link}} + L_{\mathrm{split1}} + L_{\mathrm{dec}} + L_{\mathrm{enc}} + L_{\mathrm{split2}}) - L_{\mathrm{enc}} + N_{\mathrm{hop}} G_{\mathrm{amp}} - L_{\mathrm{dec}}. \tag{5}$$

The gain for the link amplifier is chosen such that it compensates for the loss between two router nodes. Setting the maximum obtainable EDFA gain to 30 dB, we obtain the following expressions for the link optical amplifier gain:

$$G_{\mathrm{amp}} = (L_{\mathrm{link}} + L_{\mathrm{split1}} + L_{\mathrm{dec}} + L_{\mathrm{enc}} + L_{\mathrm{split2}}) \tag{6a}$$

$$G_{\mathrm{amp}} \leq 30 \text{ dB}. \tag{6b}$$

We assume that "1"s and "0"s are sent with equal probability and that the average pulse energy required by a sampling gate such as a TOAD is approximately 10 fJ. For data rates

TABLE II
LOSS CHARACTERISTICS OF THE ENCODER ARCHITECTURES

L_{enc}^{AWG}:	$2L_{AWG} + L_D = 6$ dB
L_{enc}^{TFFp}:	$6log_2(N_\lambda) + L_{TFF} + L_D$
L_{enc}^{TFFs}:	$\frac{N_\lambda + 1}{2} + L_D$

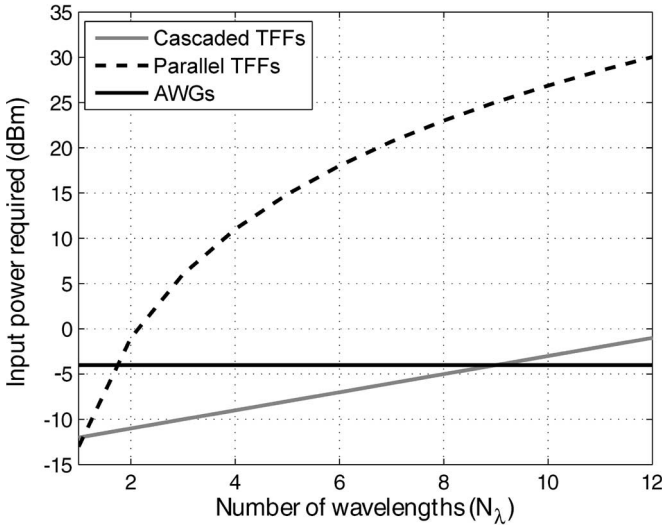

Fig. 9. Required input power versus N_λ for the three encoder/decoder architectures.

in gigahertz range, the average pulse power at the input of the gate should thus be approximately $P_{\rm rx} = -16$ dBm for accurate detection of the signal. We can now express the required transmitted signal power in terms of the encoder and decoder loss

$$P_{\rm tx} = -16 + (L_{\rm enc} + L_{\rm dec}). \tag{7}$$

The required source power and the loss between hops can be calculated using (6a) and (7). The three encoder and decoder architectures presented in the previous section (parallel TFFs, serial TFFs, and AWGs) are considered. The characteristics of the architectures are summarized in Table II, where $L_{\rm D} = 1$ dB is the delay loss, $L_{\rm enc}^{\rm TFFp}$ is the loss for the parallel TFFs encoder, $L_{\rm enc}^{\rm TFFs}$ for the serial TFFs encoder, and $L_{\rm enc}^{\rm AWG}$ for the AWG encoder. The loss for the TFF architectures is a function of the number of wavelengths N_λ, with $L_{\rm TFF} = 0.5$ dB as the loss per wavelength. This is not the case for AWGs, which have approximately uniform loss for any channel count, $L_{\rm AWG} = 2.5$ dB. For the analysis, we assume that the weight of the code equals N_λ and $L_{\rm enc} = L_{\rm dec}$.

The required input power at the station laser as a function of N_λ is shown in Fig. 9. The AWG architecture requires a source power of -4.5 dBm. Due to the extra splitting loss, the parallel TFF architecture requires an extra source power. On the other hand, the cascaded TFF architecture is more power efficient than the AWG one when the number of wavelength is $N_\lambda < 9$. The power loss between hops, which is equal to the amplifier gain (6a), depends on the splitting loss at the input and output of the router node. The broadcast operation at the input of the node splits the combined traffic by a factor of $N \times P$. At the output, P codes are recombined leading to a splitting loss of $3\log_2(P)$. The loss between hops is therefore dependent on the node degree and P. Fig. 10 shows the power loss between hops as a function of P for different architectures and degrees and for $N_\lambda = 4$. By using (6b), a bound on P can be found. We set $L_{\rm link} = 1$ dB.

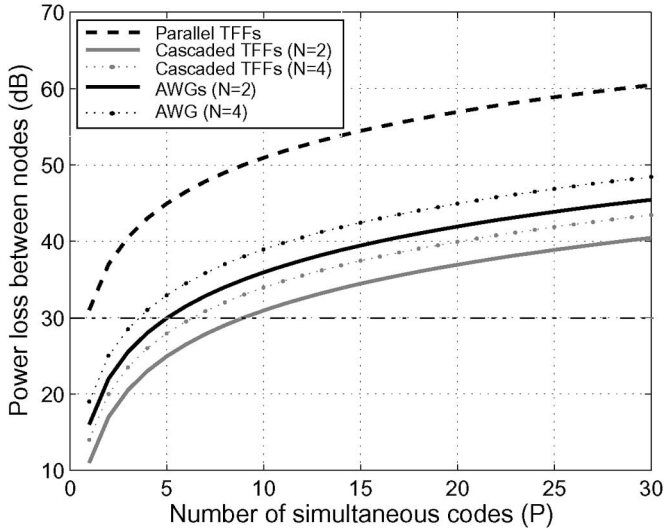

Fig. 10. Power loss between router nodes versus P for various system configurations.

As shown in Fig. 10, the parallel TFF architecture has high loss, which cannot be compensated for. The cascaded TFFs and AWG allow, respectively, for nine and five simultaneous codes on the link. As N increases, the splitting loss at the input of the router node increases, therefore diminishing the allowed value of P. However, the total traffic allowed at a node is given by $T_{\rm total} = P \times N$, assuming that all links have the same weight. For example, the total traffic allowed for $N = 2$ is $T_{\rm total} = 9 \times 2 = 18$, while for $N = 4$, $T_{\rm total} = 6 \times 4 = 24$. Even though P decreases as N increases, $T_{\rm total}$ can still increase. We will see in the following section that such values of $T_{\rm total}$ are sufficient on small area networks. At this point, we should note the difference between $T_{\rm total}$ and K, the number of simultaneous users tolerated by the OCDMA coding scheme at a specific BER. $T_{\rm total}$ is defined with respect to the power budget and is therefore an upper bound of K. The number K varies, depending on the targeted BER, but should always satisfy

$$K \le T_{\rm total} \qquad \forall\, {\rm BER}_{\rm target}. \tag{8}$$

The power budget analysis of the OCDMA multihop network gives us insights on its limitations and requirements. From our analysis, two encoder/decoder architectures satisfy the power

constraints. The cascaded TFFs architecture should be implemented when the OCDMA code uses nine wavelengths or less. For more than nine wavelengths, the AWG-based architecture gives better performance. The loss on one hop greatly depends on the splitting loss at the input and output of the router's node. As long as (8) is satisfied, P and N can be allocated differently. The effect of the degree on the network performance will be studied using simulations in the following section.

B. Simulations

While a power analysis can give a taste of the possible network limitations and can therefore be used to design the network, the routing performance and the specific advantages of an OCDMA lightwave network still need to be determined. Dynamic routing rules are more complex than static ones, but offer more flexibility. Dynamic routing algorithms are heuristic in nature, and their performance can therefore be determined through the mean of simulations. We are considering a routing algorithm that is based on Dijkstra's shortest path algorithm, which was modified to a minimum interference path algorithm taking into account interference on intranodal links. A simulator is written in Matlab to evaluate the performance of OCDMA-routed networks for various topologies and load conditions. In the simulations, an infinite number of receiving stations are attached to each node to eliminate the possibility of blocking due to a busy station: we assume that the sending station knows when the destination is busy. One or more sending stations can also be connected to the same node, depending on the network topology. Each station is modeled using a two-state Markov chain. While idle, a user has a probability of t to request a transmission. While transmitting, the user has a probability of n to stop and to go back to the idle state. At equilibrium, a user is idle $1/a = (n/t + n)$ units of time and holds a transmission for $1/b = (t/t + n)$ units of time. The user's load is given by $a/b = t/n$ Erlangs. The total offered load is $S(t/t + n)$ Erlangs, where S is the total number of transmitting stations in the network.

Dynamic routing involves choosing a path for a requested call, checking for link capacity violations, and finally assigning a virtual path to the call if the call is granted. All stations on the network start idle, and the initial maximum weights $(W^{\max})$ are calculated for each link, following the link occupancy constraint. All links start with weight $W = 0$; there are no calls on the network when the algorithm is initiated. The four steps of the algorithm for given Markov probabilities t and n are as follows.

1) Use Markov probability to start/stop transmissions for all stations on the network.
2) If start transmission:
   a) Randomly assign a destination station (d) to the transmitting stations (s).
   b) Find the minimum interference path between s and d, using modified Dijkstra's algorithm.
   c) Update the link weight along the minimum interference path: if link i is used, $W_i^{\text{new}} = W_i^{\text{old}} + 1$.
   d) If any of the link on the path has $W^{\text{new}} > W^{\max}$, call is blocked, station goes back to idle, and link weight goes back to old values.
   e) If no link on the path has $W^{\text{new}} > W^{\max}$, call is granted, and station goes to transmit.
3) If stop transmission:
   a) Update link weight along used path: if link i was used, $W_i^{\text{new}} = W_i^{\text{old}} - 1$.
   b) Station goes back to idle.
4) Go back to item 1 until set number of iteration.

The modified Dijkstra's algorithm is described below. All nodes i are assigned three parameters: a label $l(i)$ set to "1" if the node has been traversed and to "0" otherwise, a predecessor node $p(i)$ and a value $w(i)$. The source node is s, and the destination node is d. The current link weight from node i to j (number of calls already using the link $i - j$) is W_{i-j}. As a reminder, when the routing algorithm is first initiated, all weights are equal to zero. As calls are being granted, the weights increase, but are always kept below $W^{\max}$.

Initialization

For every node $i \neq s$ and node s set

- $l(i) = 0$, and $l(s) = 1$
- $w(i) = \infty$, and $w(s) = 0$
- $p(i) = 0$, and $p(s) = 0$.

Step 1)

- Find a nonpermanent node i $(l(i) = 0)$ among all temporary nodes, with the minimum weight $w(i)$.
- Set $l(i) = 1$.

Step 2)

- For every neighbor node k of i on link $i - k$, calculate the weight: $w_{\text{new}} = w(i) + (W_{i-k} - W_{p(i)-i}) + 1$.
- If $w_{\text{new}} < w(k)$, set $w(k) = w_{\text{new}}$ and $p(k) = i$.

Step 3)

- If all nodes have $l(i) = 1$, $1 \leq i \leq S$, the entire graph has been traversed. Go to Step 4).
- If some nodes have $l(i) = 0$, go back to Step 1).

Step 4)

- The path from s to d is obtained by tracing predecessors from d to s.

The values of the load t/n vary from 0.2 to 2, and the blocking probability is monitored. A simulation was run for a 20-node network and an average degree of three, the maximum degree being four and the minimum being two. The network was generated using a random graph algorithm that was implemented in Matlab. Fig. 11(a) shows the blocking probability as a function of the load per source for $K = 4$, 8, and 10. As the value of K increases, reducing the constraint on the BER per user, the blocking probability decreases, as expected. The average path lengths L^{avg} from source to destination are $L^{\text{avg}}_{K=10} = 4.0228$ hops, $L^{\text{avg}}_{K=8} = 3.9987$ hops, and $L^{\text{avg}}_{K=4} = 3.7658$ hops. The average path length increases slightly as K increases, as longer paths become available. This increase is, however, not very significant, and on average, the

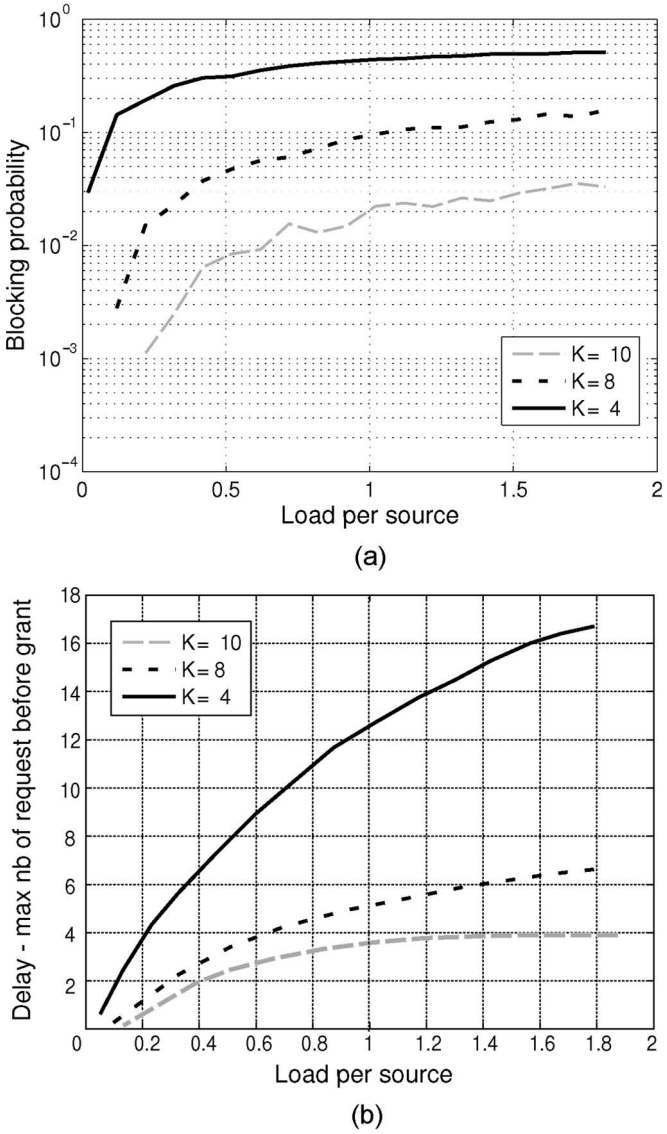

Fig. 11. Simulations of a 20-node network for $K = 10$, 8, and 4. (a) Blocking probability versus load per source. (b) Latency versus load per source.

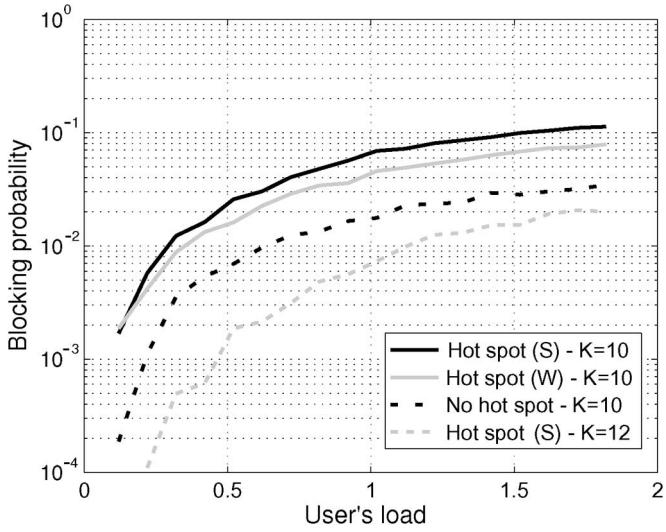

Fig. 12. Blocking probability for a 20-node network for different nonuniform traffic: S: Strong hotspot and W: Weak hotspot.

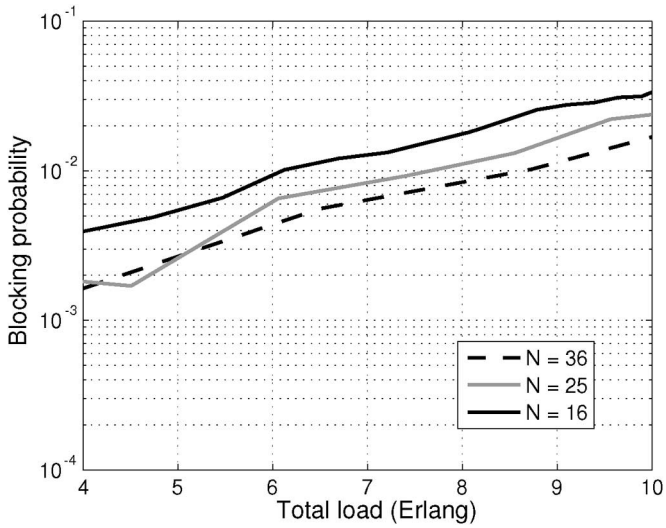

Fig. 13. Blocking probability networks with $N = 16$, 25, and 36 nodes.

path lengths are around four hops, which is far below the maximum number imposed by the noise limit from cascaded semiconductor optical amplifiers [28]. Fig. 11(b) shows the maximum number of call requests before a path is granted corresponding to the blocking probabilities in Fig. 11(a). As expected, the speed at which a call is granted is directly related to the blocking probability. This confirms that OCDMA is capable of trading BER performance for speed performance: the latency due to congestion is greatly reduced when K is increased. A first specific advantage of OCDMA is, therefore, the ability to adjust to the latency requirements of a network.

We adjusted the simulation to simulate nonuniform traffic by increasing the probability of some adjacent nodes to be chosen as destination. By directing more or less traffic toward the created bottleneck region of the network, we are able to simulate a weak (W) or strong (S) hot spots. Fig. 12 shows the blocking probability as a function of the load per source for various network conditions. For the same value of K, the blocking probability increases when a hot spot appears in the network compared to the network with uniformly distributed traffic. The links within the hot spots become fully occupied, blocking all traffic that needs to use them. Relaxing the constraints on K, allowing more calls to be granted at the price of decreased performance, can overcome the effect of the hot spot and reduce the blocking probability. A second specific advantage of OCDMA is the ability to adjust to the various network conditions and nonuniform traffic.

It was shown in a previous section that the degree of the nodes and topology will affect the routing rules. We ran simulations for networks with different number of nodes and various degrees. The results are shown in Figs. 13 and 14. In Fig. 13, the blocking probability is plotted as a function of total load in Erlangs for networks with $N = 16$, 25, and 36 nodes and $K = 8$. The average node degree of the networks

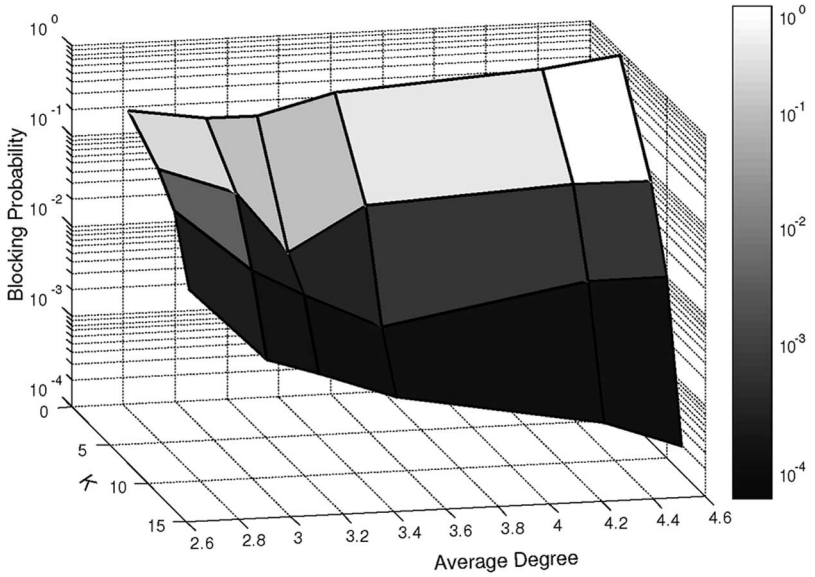

Fig. 14. Blocking probability as a function of K and average degree.

was 3, 3.2, and 3.3, respectively. The networks were all built using a similar algorithm to ensure that the connectivity was similar across all three networks and to rule out possible performance impairments due to a connectivity issue. The blocking probability increases slightly when N decreases; to achieve the same total load, the small network has to grant more calls per source. Overall, all three networks can support the same total load with an equivalent performance. We believe that code conversion, available at every node and relaxing the distinct code assignment routing rule, enables the network size to be scaled toward a larger number of nodes without affecting the blocking probabilities. As expected, the effect of the network size does impact the average path length: average path lengths increase with network size from 3.5, 4, and 4.5 hops.

We have established that the degree of each node and the connectivity of the network should also affect the routing performance of the network. As a reminder, the combination of the routing node broadcast and select architecture, and the limit on K lead to this degree/performance dependence. In order to evaluate the effect of connectivity on our routed traffic, we randomly generated multiple graphs with 20 nodes, having different average degrees, and different maximum and minimum degrees to vary the connectivity of the networks. We are presenting results from six distinct networks with average degrees of 2.7, 3, 3.2, 3.5, 4.3, and 4.6. The values of K are 4, 8, 10, and 12. All the six networks were generated to have a similar homogeneity in terms of degree per node. The results are represented in a 3-D surface plot: the blocking probability is shown as a function of both the average degree and K. We should note that the way the network is built will also have an effect on the routing, and results can vary slightly from network to network with the same average degree and max/min degree. However, these preliminary results can give us some insights on the routing/connectivity relationship.

One trend mentioned previously is once again shown in Fig. 14: blocking probability decreases when K increases. The slope of the improvement depends on the network. For understanding purposes, let us divide the networks in three categories depending on their graphs' average degree: low, medium, and high. The blocking probability improvement on networks with low average degree has the flattest slope and is the least significant. Networks with medium average degree see a significant improvement at small values of K and flattens out after a critical value of K is reached. Networks with high degree first see a slow improvement before a steep response once another critical value of K is reached. If we now consider the effect of average degree on the blocking probability, once again, we see points of inflection within the 3-D surface. The performance improves as the average degree increases until an average degree critical value is reached. The performance then decreases.

These trends can be explained as follows.

1) A network with a low average degree has few links and, therefore, few possible paths. Increasing the value of K, thus, has a limited effect as the main source of blockage comes from the limited amount of paths (path-limited region).
2) A network with a high average degree has many possible paths within the network. A low value of K is not sufficient to allow traffic on all links if we recall that the number of codes that is allowed on link i with degree N^i is K/N^i. At low values of K, the network performance is therefore limited by K itself (K-limited region). When the critical value K^1_{crit} is reached, the network is no longer in the K-limited region, and the performance increases significantly.
3) A network with a medium average degree combines both effects: the critical value K^1_{crit} is lower than for high average degree so that the performance increases significantly when K is first increased. However, when the second critical value K^2_{crit} is reached, the network then falls in the path-limited region of operation.

4) When considering a constant K, increasing the average degree means more paths and, therefore, an increased performance until the critical value $\mathrm{Deg}_{\mathrm{crit}}$. At this point, the network enters the K-limited region, and the performance starts decreasing when the average degree increases. For higher value of K, $\mathrm{Deg}_{\mathrm{crit}}$ increases. For example, in Fig. 14, $\mathrm{Deg}_{\mathrm{crit}}$ for $K = 4$, 8, 10, and 12 is 3, 3.2, 3.5, and 4.6, respectively.

We should also note that, for the same average degree, a network with a highest degree homogeneity will perform better than with a lower degree homogeneity, as no bottlenecks are created within the network.

V. Discussion and Conclusion

In this paper, we presented the architecture and analysis of OCDMA lightwave networks. The main focus of this paper was to explore the use of OCDMA in multihop networks and to understand how OCDMA properties can be utilized. The network analysis was developed to identify the operation limits of such lightwave networks. A simulator was written to evaluate the performance of the network when routing is performed using a minimum interference routing algorithm. The routing rules, which are very unique to OCDMA networks, are presented. For all our simulated graphs, local area or access networks are considered: small number of nodes and low average degrees. In these situations, the OCDMA networks show good performance and flexibility. The noise and loss impose limits on the maximum number of hops and maximum number of codes K, respectively. However, from our simulations, an OCDMA network with low average degree and low values of K can route a call to its destination without reaching the loss and noise limits.

OCDMA offers flexibility with coding, large cardinality, and the code conversion. OCDMA coding creates a soft limit in terms of a number of users, allowing the network to operate at different levels of BER performance. We have shown that this is an important advantage of OCDMA systems; the network can easily be adapted to various networking requirements or load conditions, which might not be feasible in more rigid WDM-based networks. Dynamic networks can therefore benefit from the OCDMA routing. A large offered cardinality is also an advantage of the OCDMA: powerful 2-D coding can be used to create a large pool of codes while using few wavelengths. This increased granularity eliminates many routing impairments. The code conversion adds another level of flexibility by creating VCPs. The routing rules are therefore simplified: a call can be granted as soon as a path is available, code availability not being a constraint.

References

[1] C.-S. Brès, Y.-K. Huang, I. Glesk, and P. R. Prucnal, "Scalable asynchronous incoherent optical CDMA," *J. Opt. Netw.*, vol. 6, no. 6, pp. 599–615, Jun. 2007.

[2] J. Shah, "Optical CDMA," *Opt. Photon. News*, vol. 14, no. 4, pp. 42–47, Apr. 2003.

[3] A. Stok and E. Sargent, "The role of optical CDMA in access networks," *IEEE Commun. Mag.*, vol. 40, no. 9, pp. 409–411, Sep. 2002.

[4] D. Zaccarin and M. Kavegard, "An optical CDMA system based on spectral amplitude encoding of an LED," *IEEE Photon. Technol. Lett.*, vol. 4, no. 4, pp. 479–482, 1993.

[5] A. Hassan, J. Hershey, and N. Riza, "Spatial optical CDMA," *IEEE J. Sel. Areas Commun.*, vol. 13, no. 3, pp. 609–613, Apr. 1995.

[6] P. Prucnal, M. Santoro, and T. Fan, "Spread spectrum fiber-optic local area network using optical processing," *Electron. Lett.*, vol. 4, no. 5, pp. 547–554, May 1986.

[7] L. Tancevski and I. Andonovic, "Wavelength hopping/time spreading code division multiple access systems," *Electron. Lett.*, vol. 30, no. 9, pp. 721–723, 1994.

[8] G. Yang and W. Kwong, "Two-dimensional spatial signature patterns," *IEEE Trans. Commun.*, vol. 44, no. 2, pp. 184–191, Feb. 1996.

[9] R. Yim, L. Chen, and J. Bajcsy, "Design and performance of 2-D codes for wavelength-time optical CDMA," *IEEE Photon. Technol. Lett.*, vol. 14, no. 5, pp. 714–716, May 2002.

[10] T. Okuno, M. Onishi, and M. Nishimura, "Generation of an ultra-broadband supercontinuum by dispersion-flattened and decreasing fiber," *IEEE Photon. Technol. Lett.*, vol. 10, no. 1, pp. 72–74, Jan. 1998.

[11] S. Kim, M. Kang, S. Park, Y. Choi, and S. Han, "Incoherent bidirectional fiber-optic code division multiple access networks," *IEEE Photon. Technol. Lett.*, vol. 12, no. 7, pp. 921–923, Jul. 2000.

[12] L. Chen, "Technologies for hybrid wavelength-time optical CDMA transmission," in *Proc. Can. Conf. Elect. and Comput. Eng.*, 2001, vol. 1, pp. 435–440.

[13] Y.-K. Huang, V. Baby, P. Prucnal, C. Greiner, D. Iazikov, and T. Mossberg, "Integrated holographic encoder for wavelength-hopping/time-spreading optical CDMA," *IEEE Photon. Technol. Lett.*, vol. 17, no. 4, pp. 825–827, Apr. 2005.

[14] L. Chen and P. Smith, "Demonstration of incoherent wavelength-encoding/time-spreading optical CDMA using chirped moire gratings," *IEEE Photon. Technol. Lett.*, vol. 12, no. 9, pp. 1281–1283, Sep. 2000.

[15] *Little Optics Inc. White Paper: Economics of Very Large Scale Integration Photonics*, Mar. 2003.

[16] P. Prucnal, M. Krol, and J. Stacy, "Demonstration of a rapidly tunable optical time-division multiple-access coder," *IEEE Photon. Technol. Lett.*, vol. 4, no. 2, pp. 170–172, Feb. 1991.

[17] K.-L. Deng, K. Kang, I. Glesk, and P. Prucnal, "A 1024-channel fast tunable delay line for ultrafast all-optical TDM networks," *IEEE Photon. Technol. Lett.*, vol. 9, no. 11, pp. 1496–1498, Nov. 1997.

[18] C. Lam, "To spread or not to spread—The myths of optical CDMA," in *Proc. IEEE LEOS Annu. Meeting*, Oct. 2000, vol. 2, pp. 13–16.

[19] N. Doran and D. Wood, "Nonlinear-optical loop mirror," *Opt. Lett.*, vol. 13, no. 1, pp. 56–58, Jan. 1988.

[20] J. Lee, P. Teh, P. Petropoulos, M. Ibsen, and D. Richardson, "A grating-based OCDMA coding-decoding system incorporating a nonlinear optical loop mirror for improved code recognition and noise reduction," *J. Lightw. Technol.*, vol. 20, no. 1, pp. 36–46, Jan. 2002.

[21] J. Sokoloff, P. Prucnal, I. Glesk, and M. Kane, "A terahertz optical asymmetric demultiplexer (TOAD)," *IEEE Photon. Technol. Lett.*, vol. 5, no. 7, pp. 787–790, Jul. 1993.

[22] L. Xu, I. GLesk, V. Baby, and P. Prucnal, "Multiple access interference (MAI) noise reduction in a 2D optical CDMA system using ultrafast optical thresholding," in *Proc. LEOS Annu. Meeting*, 2004, pp. 591–592.

[23] C.-S. Brès, I. Glesk, and P. Prucnal, "Demonstration of a transparent router for wavelength-hopping time-spreading optical CDMA," *Opt. Commun.*, vol. 254, no. 1, pp. 58–66, Oct. 2005.

[24] W. Kwong and G.-C. Yang, *Prime Codes With Applications to CDMA Optical and Wireless*. Boston, MA: Artech House.

[25] L. Tancevski, M. Tur, J. Budin, and I. Andonovic, "Hybrid wavelength hopping/time spreading code division multiple access systems," *Proc. Inst. Electr. Eng.—Optoelectronics*, vol. 143, no. 3, pp. 161–166, Jun. 1996.

[26] K. Yu and N. Park, "Design of new family of two-dimensional wavelength-time spreading codes for optical code division multiple access networks," *Electron. Lett.*, vol. 35, no. 10, pp. 830–831, May 1999.

[27] W.-C. Kwong and G.-C. Yang, "Extended carrier-hopping prime codes for wavelength-time optical code-division multiple access," *IEEE Trans. Commun.*, vol. 52, no. 7, pp. 1084–1098, Jul. 2004.

[28] O. Liboiron-Ladouceur, M. Boroditsky, K. Bergman, and M. Brodsky, "Polarization-dependent gain in SOA-based optical multistage interconnection networks," *J. Lightw. Technol.*, vol. 24, no. 11, pp. 3959–3967, Nov. 2006.

Camille-Sophie Brès (S'03) received the B.Eng. degree (with honors) in electrical engineering from McGill University, Montreal, QC, Canada, in 2002 and the M.S. and Ph.D. degrees from the Department of Electrical Engineering, Princeton University, Princeton, NJ, in 2004 and 2007, respectively. Her graduate research work involved all-optical network and system design based upon OCDMA technologies and nonlinear optics.

She is currently a Postdoctoral Researcher with the Department of Computer and Electrical Engineering, University of California, San Diego, La Jolla, where she is involved in the development of parametric and nonlinear processes for ultrafast optical processing.

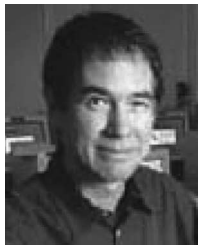

Paul R. Prucnal (S'75–M'78–SM'90–F'92) received the A.B. degree from Bowdoin College, Brunswick, ME, in 1974 and the M.S., M.Phil., and Ph.D. degrees from Columbia University, New York, NY, in 1976, 1978, and 1979, respectively.

Since 1988, he has been with Princeton University, Princeton, NJ, as a Professor of electrical engineering. He was the founding Director of Princeton's Center for Photonics and Optoelectronic Materials. He is currently the Director of Princeton's Center for Networks Research and Applications. He has authored or coauthored some 250 journal articles/book chapters and is the holder of 17 U.S. patents.

Prof. Prucnal is an Area Editor of the IEEE TRANSACTIONS ON COMMUNICATIONS. He is a Fellow of the Optical Society of America and a member of Phi Beta Kappa, Eta Kappa, and Sigma Xi. He was the recipient of the 1990 Rudolf Kingslake Medal from the International Society of Optical Engineering and received the Gold Medal from the Faculty of Mathematics, Physics, and Informatics from Comenius University in 2006.